




Simulation of Low Velocity Impact on CFRP Aerospace Structures: Simplified Approaches, Numerical and Experimental Results

V. Prentzias¹  · G. J. Tsamasphyros¹

Received: 21 November 2018 / Accepted: 6 December 2018 / Published online: 19 December 2018
© Springer Nature B.V. 2018

Abstract

This paper presents a study of low velocity impact on unidirectional composite specimens, a plate and an aerospace stiffened panel following the building block approach. Simplified approaches for a quick estimation of impact behavior description are used to define the impact dynamic response and the existence of delamination at coupon level, while numerical analysis models using ABAQUS/Explicit software and experimental results are described in detail and compared at all levels. Significant effort was made in the use of different types of elements and damage models for matrix cracking, fiber breakage and cohesive elements for delamination between plies of composite. The results obtained show that simplified approaches give an effective initial understanding of the impact response helping the interpretation of numerical and experimental results. In addition, the comparison of different methods of simulation demonstrated that continuum shell elements with induced cohesive elements present the most accurate results regarding the impact force, contact duration, energy absorption and damage extension.

Keywords A. Low velocity impact · B. Explicit finite element analysis · C. Interlaminar damage · D. Intralaminar damage · E. Aerospace CFRP panels · F. Building block approach

1 Introduction

The use of polymer-based composites reinforced by carbon fibers in aerospace industry has been significantly increased over the last decades. The main reason of this fact is their improved mechanical properties of unit mass, the capability of flexible design in relevance with their low cost and their reduced environmental impact. As a result, extensive work has been performed in order to evaluate the mechanical behavior of various types of composite structures under different loads. One of the most challenging and complex case of mechanical behavior is

✉ V. Prentzias
chm11005@central.ntua.gr

¹ Strength of Materials Laboratory, National Technical University of Athens, 5 Iroon Polytechniou, Zographou, GR 157 73 Athens, Greece

impact of foreign objects on aerospace structures [1, 2] and especially on composite in relation with their dynamic response and also the evaluation of possible caused damage [3].

The definition of impact damage in composite materials is related to the definition and interaction of different failure modes like matrix cracking, fiber breakage, debonding and delamination. When we need to evaluate the possible type of damage we have primarily to examine the effect of many parameters that influence the impact event e.g. geometry and material properties of the structure and the impactor, drop weight mass and velocity. In addition, the use of only simplified models to describe the impact event on a certain configuration will help us to develop efficient numerical models and experimental tests. Although, many researchers have used analytical closed [4, 5] and semi-closed form solutions for describing an impact event, it has been proved that these methods are only applicable to very simple cases. As a result, these methods provide a better understanding of the controlling factors of an impact without being suitable for predicting damages like delamination and matrix cracking. In recent work of Soutis C. et al. [6–8] cohesive zone elements were used not only for delamination but also for matrix cracking and splitting that impact upon the triggering of delamination and hence energy absorbed.

In case that we want to check if damage occurs due to low velocity impact at simple structures of composite materials, impact force is defined using simplified mechanical models. The maximum value of this force is then compared with a critical value of the relevant mode of damage e.g. delamination [9–13].

The scope of this paper is to study, according to the building block approach the behavior of composite specimens, a composite plate and an aerospace stiffened composite panel due to impact using advanced simulation techniques. To the authors' knowledge there is a lack of published literature with comparison of the behavior of different element types and damage models under impact loading verified not only with experimental results but also with their application to all levels of building block approach leading to real aerospace composite structures. As a result, a detail work has been executed in order to examine the behavior of various element types and damage numerical models under low velocity impact. In addition, this study is accompanied with a quick estimation tool in coupon level while the most accurate simulation method is implemented in larger scale composite structures.

2 Approach for Low Velocity Impact Behavior Description

According to Olsson [4, 14] and Gonzalez and al. [15] when $M_{impactor}/M_{plate} \geq 2$ the behavior of the composite plate in low velocity impact is called quasi-static which is a size and boundary controlled response. The following loads are considered in the quasi-static model:

- a) The inertial load of the impactor F_i

$$F_i = -M_i \ddot{w}_i \quad (1)$$

where M_i , w_i are the impactor mass and displacement respectively.

- b) The contact load F_c for the description of local deflections is considered with the use of the contact law

$$F_c = k_a a^q \quad (2)$$

where k_α is the contact stiffness, α is the indentation of the impactor to the plate with $\alpha = w_i - w_o$ the difference between displacements of impactor and plate mid-plane, q is a power parameter. We consider $q = 1$ for linear contact law and $k_\alpha = 5.2RY_C$ [15, 16], where R is impactor radius and Y_C is ply transverse strength under compression.

c) The plate deflection load F_o can be approached as [17]

$$F_o = k_{bs}w_o \tag{3}$$

where k_{bs} is the bending-shearing stiffness of the plate. Assuming simply supported boundary conditions we have $k_{bs} = D^*/(0.0116b^2)$ [18], where b is the small edge length of the plate [19, 20] and D^* the effective bending stiffness of the laminate [9, 14]:

$$D^* \approx \sqrt{\left(\frac{A+1}{2}D_{11}D_{22}\right)}, \quad A = \frac{D_{12} + 2D_{66}}{\sqrt{D_{11}D_{22}}} \tag{4}$$

Under equilibrium ($F_i = F_c = F_o$), we derive the following simplified equation for quasi-static behavior:

$$\left(1 + \frac{k_a}{k_{bs}}\right)\ddot{a} + \frac{k_a}{M_i}a = 0, \quad \dot{a}_o = \frac{k_{bs}}{k_a + k_{bs}}V_o, \quad a_o = 0 \tag{5}$$

In accordance with Christoforou and Yigit [18, 21] after solving the equilibrium differential Eq. (5), impact force versus time is given by the relation

$$F(t) = V_o\sqrt{M_iK_a}\sqrt{\frac{\lambda}{\lambda+1}}\sin\left(\sqrt{\frac{\lambda}{\lambda+1}}\omega t\right) \tag{6}$$

while impactor displacement versus time is given by the following relation

$$w_i(t) = \frac{V_o}{\omega}\sqrt{\frac{\lambda+1}{\lambda}}\sin\left(\sqrt{\frac{\lambda}{\lambda+1}}\omega t\right) \tag{7}$$

where $\lambda = K_{bs}/K_\alpha$ is the relative stiffness of the plate and $\omega = \sqrt{\frac{K_a}{M_i}}$ is called linear contact frequency.

Generally, in low velocity impact matrix cracks act only as areas of delamination initiation between different oriented composite plies and do not reduce the stiffness of a structure. A delamination is a severe damage mode because it mainly reduces the compressive strength of a composite laminate.

A criterion for the growth of n_d number of delaminations in a composite plate under static conditions, or dynamic cases like impact with an acceptable deviation, has been developed by Olsson et al. [19]. The critical value is given by the equation:

$$F_{dn_d}^{stat} = \pi\sqrt{\frac{32D^*G_{IIc}}{n_d + 2}} \tag{8}$$

where D^* is the effective bending stiffness of the plate and G_{IIc} is the fracture toughness in pure mode II.

3 Damage Models

3.1 Intralaminar Damage Model

3.1.1 Hashin 2D Model

Initiation Many damage models have been developed in order to evaluate the type and extent of a failure for matrix and fiber inside the ply of a composite subjected to an external loading condition. One of the most widely known intralaminar damage model for composite materials which refer to the following four different type of damage is Hashin [22, 23]:

$$\text{Fiber tension}(\hat{\sigma}_{11} \geq 0) : F_f^t = \left(\frac{\hat{\sigma}_{11}}{X^T} \right) + a \left(\frac{\hat{\tau}_{12}}{S^L} \right)^2 \quad (9)$$

$$\text{Fiber compression}(\hat{\sigma}_{11} < 0) \quad F_f^c = \left(\frac{\hat{\sigma}_{11}}{X^C} \right)^2 \quad (10)$$

$$\text{Matrix tension}(\hat{\sigma}_{22} \geq 0) \quad F_m^t = \left(\frac{\hat{\sigma}_{22}}{Y^T} \right)^2 + \left(\frac{\hat{\tau}_{12}}{S^L} \right)^2 \quad (11)$$

$$\text{Matrix compression} (\hat{\sigma}_{22} < 0) \quad F_m^c = \left(\frac{\hat{\sigma}_{22}}{2S^T} \right)^2 + \left[\left(\frac{Y^C}{2S^L} \right)^2 - 1 \right] \frac{\hat{\sigma}_{22}}{Y^C} + \left(\frac{\hat{\tau}_{12}}{S^L} \right)^2 \quad (12)$$

In the above equations X^T is the longitudinal tensile strength of the ply, X^C is the longitudinal compressive strength, Y^T is the transverse tensile strength, Y^C is the transverse compressive strength, S^L longitudinal shear strength, S^T transverse shear strength, α is a coefficient that defines the contribution of shear stress to the fiber tension criterion and $\hat{\sigma}_{11}, \hat{\sigma}_{22}, \hat{\tau}_{12}$ are the elements of the effective stress tensor $\hat{\sigma}$ which are used for the evaluation of initiation criteria according to the relation:

$$\hat{\sigma} = M\sigma \quad (13)$$

where σ is the tensor of real stress and M is the damage matrix:

$$M = \begin{bmatrix} \frac{1}{(1-d_f)} & 0 & 0 \\ 0 & \frac{1}{(1-d_m)} & 0 \\ 0 & 0 & \frac{1}{(1-d_s)} \end{bmatrix} \quad (14)$$

with d_f , d_m and d_s the damage variables that characterize the damages of fiber, matrix and shear. These variables are defined from the values d_f^t , d_f^c , d_m^t and d_m^c which are relevant to the four different mode of failure according to:

- $$d_f = d_f^t \text{ if } \hat{\sigma}_{11} \geq 0 \text{ or } d_f = d_f^c \text{ if } \hat{\sigma}_{11} < 0 \tag{15}$$

- $$d_m = d_m^t \text{ if } \hat{\sigma}_{22} \geq 0 \text{ or } d_m = d_m^c \text{ if } \hat{\sigma}_{22} < 0 \tag{16}$$

- $$d_s = 1 - \left(1 - d_f^t\right) \left(1 - d_f^c\right) \left(1 - d_m^t\right) \left(1 - d_m^c\right) \tag{17}$$

Finally, before any initiation and evolution of damage the damage matrix M is equal to the unit matrix and then $\hat{\sigma} = \sigma$.

Evolution Damage evolution refers to the behavior of material after the initiation of damage and gives the rate of degradation of its stiffness. While initially the response of the material is linear elastic, after the creation of damage it is given by the equation:

$$\sigma = C_d \varepsilon \tag{18}$$

where ε is the strain value and C_d is the damaged elasticity matrix defined as

$$C_d = \frac{1}{D} \begin{bmatrix} (1-d_f)E_1 & (1-d_f)(1-d_m)v_{21}E_1 & 0 \\ (1-d_f)(1-d_m)v_{12}E_2 & (1-d_m)E_2 & 0 \\ 0 & 0 & (1-d_s)GD \end{bmatrix} \tag{19}$$

where $D = 1 - (1 - d_f)(1 - d_m)v_{12}v_{21}$, d_f reflects the current state of fiber damage, d_m reflects the current state of matrix damage, d_s reflects the current state of shear damage, E_1 is the Young’s modulus in the fiber direction, E_2 is the Young’s modulus in the matrix direction, G is the shear modulus, and v_{12} and v_{21} are Poisson’s ratios.

After damage initiation ($\delta_{eq} \geq \delta_{eq}^o$) the damage variable for a certain mode is defined as

$$d = \frac{\delta_{eq}^f \left(\delta_{eq} - \delta_{eq}^o \right)}{\delta_{eq} \left(\delta_{eq}^f - \delta_{eq}^o \right)} \tag{20}$$

where δ_{eq}^o is the initial equivalent displacement at which the initiation criterion for that mode is met and δ_{eq}^f is the displacement at which the material is completely damaged in this failure mode. It is known as linear damage evolution and for each failure mode the energy dissipated due to failure G^c must be specified.

3.1.2 Hashin 3D – Puck Model [24]

Firstly, the constitutive equation for an elastic orthotropic material is described as:

$$\begin{bmatrix} \sigma_{11} \\ \sigma_{22} \\ \sigma_{33} \\ \sigma_{12} \\ \sigma_{23} \\ \sigma_{31} \end{bmatrix} = \begin{bmatrix} C_{11} & C_{12} & C_{13} & 0 & 0 & 0 \\ C_{12} & C_{22} & C_{23} & 0 & 0 & 0 \\ C_{13} & C_{23} & C_{33} & 0 & 0 & 0 \\ 0 & 0 & 0 & 2G_{12} & 0 & 0 \\ 0 & 0 & 0 & 0 & 2G_{23} & 0 \\ 0 & 0 & 0 & 0 & 0 & 2G_{31} \end{bmatrix} \begin{bmatrix} \varepsilon_{11} \\ \varepsilon_{22} \\ \varepsilon_{33} \\ \varepsilon_{12} \\ \varepsilon_{23} \\ \varepsilon_{31} \end{bmatrix} \tag{21}$$

In case of damage existence four different variables are introduced:

- Two variables in relation for fibers in tension and compression: d_{ft} , d_{fc}
- Two variables in relation for matrix in tension and compression d_{mt} , d_{mc}

These different four damage variables are used in order to define the total damage values for both fiber and matrix of the composite material according to the following relations:

$$d_f = 1 - (1 - d_{ft})(1 - d_{fc}) \tag{22}$$

$$d_m = 1 - (1 - d_{mt})(1 - d_{mc}) \tag{23}$$

The elastic constants C_{ij} when damage exists are calculated in relevance with the respective constants when damage has not been appeared yet in the material and also the above damage variables:

$$\begin{aligned} C_{11} &= (1 - d_f) C_{11}^0 \\ C_{22} &= (1 - d_f)(1 - d_m) C_{22}^0 \\ C_{33} &= (1 - d_f)(1 - d_m) C_{33}^0 \\ C_{12} &= (1 - d_f)(1 - d_m) C_{12}^0 \\ C_{13} &= (1 - d_f)(1 - d_m) C_{13}^0 \\ C_{22} &= (1 - d_f)(1 - d_m) C_{22}^0 \\ G_{12} &= (1 - d_f)(1 - s_{mt}d_{mt})(1 - s_{mc}d_{mc}) G_{12}^0 \\ G_{23} &= (1 - d_f)(1 - s_{mt}d_{mt})(1 - s_{mc}d_{mc}) G_{23}^0 \\ G_{31} &= (1 - d_f)(1 - s_{mt}d_{mt})(1 - s_{mc}d_{mc}) G_{31}^0 \end{aligned} \tag{24}$$

The s_{mt} $\kappa \alpha \iota$ s_{mc} coefficients control the loss of shear stiffness due to the damage of matrix in tension and compression respectively.

The elastic constants in the case of composite material without any type of damage are functions of Young modulus of elasticity and Poisson ratio defined as

$$\begin{aligned} C_{11}^0 &= E_{11}^0(1 - \nu_{23}\nu_{32})\Gamma \\ C_{22}^0 &= E_{22}^0(1 - \nu_{13}\nu_{31})\Gamma \\ C_{33}^0 &= E_{33}^0(1 - \nu_{12}\nu_{21})\Gamma \\ C_{12}^0 &= E_{11}^0(\nu_{21} + \nu_{31}\nu_{23})\Gamma \\ C_{23}^0 &= E_{22}^0(\nu_{32} + \nu_{12}\nu_{31})\Gamma \\ C_{13}^0 &= E_{11}^0(\nu_{31} + \nu_{21}\nu_{32})\Gamma \end{aligned} \tag{25}$$

where $\Gamma = 1 / (1 - \nu_{12}\nu_{21} - \nu_{23}\nu_{32} - \nu_{31}\nu_{13} - 2\nu_{21}\nu_{32}\nu_{13})$

The damage variables which are related to failure of fiber tension, fiber compression, matrix tension and matrix compression are equal to one when the relevant failure criterion is reached. Combining Hashin 3D model for fiber damage and Puck [25, 26] model for matrix damage the following equations are used:

Tensile fiber mode where $s_{11} > 0$:

$$\text{If } \left(\frac{\sigma_{11}}{X_{1t}}\right)^2 + \left(\frac{\sigma_{12}}{S_{12}}\right)^2 + \left(\frac{\sigma_{13}}{S_{13}}\right)^2 = 1, d_{ft} = 1 \tag{26}$$

Compressive fiber mode where $s_{11} < 0$:

$$\text{If } \frac{|\sigma_{11}|}{X_{1c}} = 1, d_{fc} = 1 \tag{27}$$

Tensile and compressive matrix mode:

$$\left[\left(\frac{\sigma_{11}}{2X_{1t}}\right)^2 + \frac{\sigma_{22}^2}{|X_{2t}X_{2c}|} + \left(\frac{\sigma_{12}}{S_{12}}\right)^2 \right] + \sigma_{22} \left(\frac{1}{X_{2t}} + \frac{1}{X_{2c}}\right) = 1 \text{ and :} \tag{28}$$

$$\sigma_{22} + \sigma_{33} > 0, d_{mt} = 1$$

$$\sigma_{22} + \sigma_{33} < 0, d_{mc} = 1$$

The following material constants have been introduced in the previous equations:

X_{1t} = tensile failure stress in fiber direction, X_{1c} = compressive failure stress in fiber direction, X_{2t} = tensile failure stress in direction 2 (transverse to fiber direction), X_{2c} = compressive failure stress in direction 2 (transverse to fiber direction), X_{3t} = tensile failure stress in direction 3 (transverse to fiber direction), X_{3c} = compressive failure stress in direction 3 (transverse to fiber direction), S_{12} = failure shear stress in 1–2 plane, S_{13} = failure shear stress in 1–3 plane, S_{23} = failure shear stress in 2–3 plane.

3.2 Interlaminar Damage Model

3.2.1 Initiation

In order to evaluate the initiation of damage between the plies of a composite layup with the use of cohesive elements there is a criterion named quadratic nominal stress criterion defined from traction – separation law.

Damage is assumed to initiate when a quadratic interaction function involving the nominal stress ratios reaches a value of one. This criterion is called Quads [23] and can be represented as

$$\left\{ \frac{\langle t_n \rangle}{t_n^o} \right\}^2 + \left\{ \frac{\langle t_s \rangle}{t_s^o} \right\}^2 + \left\{ \frac{\langle t_t \rangle}{t_t^o} \right\}^2 = 1 \tag{29}$$

where t_n^o, t_s^o , and t_t^o represent the peak values of the nominal stress when the deformation is either purely normal to the interface or purely in the first or the second shear direction, respectively.

3.2.2 Propagation

The damage evolution law [23] describes the rate at which the material stiffness is degraded once the corresponding initiation criterion is reached. Damage evolution can be defined based on the energy that is dissipated as a result of the damage process, also called the fracture energy. The fracture energy is equal to the area under the traction-separation curve.

Power Law Form The dependence of the fracture energy on the mode mix can be defined based on a power law fracture criterion. The power law criterion states that failure under mixed-mode conditions is governed by a power law interaction of the energies required to cause failure in the individual (normal and two shear) modes. It is given by

$$\left\{ \frac{G_n}{G_n^c} \right\}^a + \left\{ \frac{G_s}{G_s^c} \right\}^a + \left\{ \frac{G_t}{G_t^c} \right\}^a = 1 \quad (30)$$

with the mixed-mode fracture energy $G^c = G_n + G_s + G_t$ when the above condition is satisfied. In the expression above the quantities G_n , G_s , G_t refer to the work done by the traction and its conjugate relative displacement in the normal, the first, and the second shear directions, respectively. You specify the quantities G_n^c , G_s^c , G_t^c which refer to the critical fracture energies required to cause failure in the normal, the first, and the second shear directions, respectively.

Benzeggagh-Kenane (B-K) Form The Benzeggagh-Kenane fracture criterion [23] is particularly useful when the critical fracture energies during deformation purely along the first and the second shear directions are the same; i.e., $G_s^c = G_t^c$. It is given by the equation

$$G_n^c + (G_s^c - G_n^c) \left\{ \frac{G_s}{G_t} \right\} = G^c \quad (31)$$

where $G_S = G_s + G_t$, $G_T = G_n + G_S$ and n is a material parameter.

4 Laminated Composite Specimens

4.1 Numerical Impact Modeling

The experimental impact tests presented below were modelled in Abaqus/CAE and analyzed using Abaqus/Explicit. All presented models have been run in a Sun Blade X6440 server module (PC cluster) of four Six Core Opteron processors (24 CPUs) with 96 GB RAM totally. The material properties used for all the numerical simulations for composite layers of specimens are reported in Table 1 [15, 27].

Laminated composites were made using a symmetric balanced layup of $[45_4/0_4/-45_4/90_4]_s$ (with the fiber oriented in the longer specimen side) with ply material Hexply AS4/8552. The numerical models were simplified to reduce the analysis execution time and only a part of the specimen inside the fixture was modelled (125 mm × 75 mm). The used boundary conditions and external loads are reported in Fig. 1.

Table 1 Material properties

Ply mechanical properties Hexply AS4/8552

Density	$1590 \times 10^{-9} \text{ kg/mm}^3$
Ply thickness	$t = 0.18125 \text{ mm}$
Elastic properties	$E_{11} = 128.0 \text{ GPa}, E_{22} = 7.6 \text{ GPa}, G_{12} = 4.4 \text{ GPa}, \nu_{12} = 0.35, \nu_{23} = 0.45$
Ply strength properties	$X_T = 2300.0 \text{ MPa}, X_c = 1531.0 \text{ MPa}, Y_T = 26.0 \text{ MPa}, Y_c = 199.8 \text{ MPa}, S_L = 78.4 \text{ MPa}, S_T = 78.4 \text{ MPa}$

After a comparison of different methodologies that is described in detail later in the section of results and discussion, more accurate simulation for laminated composite specimens was performed with the use of continuum shell elements. They were created with eight sublaminates of continuum shell elements (SC8R) through the thickness using advanced techniques currently available in Abaqus for layup definition. The interlayer damage (delamination) was considered using six layers of cohesive elements (COH3D8) of zero thickness using shared nodes method using Quads criterion for damage initiation and Power law ($a = 1$) for damage propagation. Finally, the intralayer damage (matrix cracking and fiber failure) was simulated using Abaqus built-in Hashin damage model for damage initiation and linear energy law for damage propagation [23].

The impactor deformations were very small compare to the composite so they were not considered in the FE model. For these reasons the impactor is modelled with rigid elements (R3D4) available in Abaqus which help to reduce the total computational time.

When general contact with hard contact law was used between the surfaces of the impactor and the specimen, spikes with very high magnitudes appeared in the contact

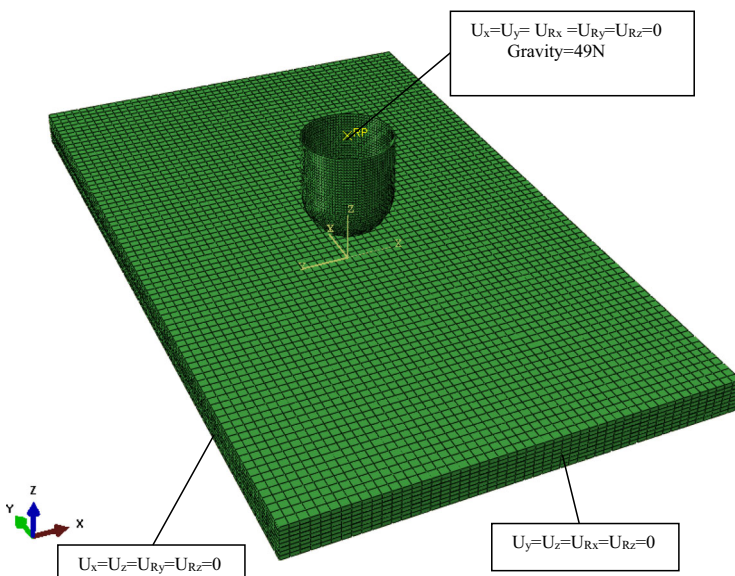


Fig. 1 Boundary conditions used in the Finite Element model of specimens

force. Alternatively, a pressure–overclosure method based on the Hertzian contact theory was implemented according to the following equation [28]:

$$p = \frac{3k_H y^{\frac{1}{2}}}{4\pi R} \quad (32)$$

where p is the contact pressure, y is the overclosure (penetration) of the slave nodes (nodes of the impactor), R is impactor radius and k_H is the contact stiffness which for a transversely isotropic material is (Olsson) [16]:

$$K_H = \frac{4}{3} Q \sqrt{R} \quad (33)$$

Q is the effective out-of-plane stiffness and given by:

$$\frac{1}{Q} = \frac{1}{Q_p} + \frac{1}{Q_i} \quad (34)$$

where

$$Q_z = E_z / (1 - \nu_r \nu_z) \quad (35)$$

Subscripts i and p refer to the impactor and the plate and subscripts r and z refer to the in-plane and out-of-plane directions, respectively.

4.2 Experimental Tests

The impact model technique presented above was tested using different experimental tests from literature. An experimental test case of impact on a composite flat plate made by carbon fiber/epoxy [15] has been reported here.

Rectangular flat specimens of 150 mm × 100 mm have been impacted with a hemispherical ($r = 8$ mm) impactor of 5 kg following the ASTM standard D7136 [29]. Two impact energies values were used (Table 2).

5 Laminated Composite Plate

5.1 Numerical Impact Modeling

Consider the flat CFRP plate 300 mm × 300 mm shown in Fig. 2 which is manufactured with plies of UD composite material IM7–8552 (by Hexcel) (Table 3) [30].

Table 2 Impact tests

Coupon	Impact energy (J)	Impactor velocity (ms ⁻¹)
L04-S01	38.6	3.93
L04-S04	28.6	3.38

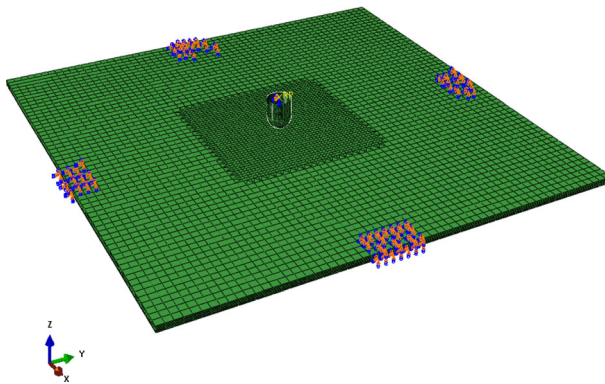


Fig. 2 Boundary conditions used in the Finite Element model of plate

In detail, the layout of the plate was consisted of the following 28 plies $[45^\circ / 90^\circ / -45^\circ / 0^\circ / 45^\circ / 90^\circ / -45^\circ / 0^\circ / 0^\circ / -45^\circ / 90^\circ / 45^\circ / 0^\circ / -45^\circ / 90^\circ / 45^\circ / 0^\circ / -45^\circ / 90^\circ / 45^\circ / 0^\circ / 90^\circ / 0^\circ / 90^\circ / 0^\circ / -45^\circ / 45^\circ]$.

The experimental impact tests presented above were modelled in Abaqus/CAE and analyzed using Abaqus/Explicit. The model was built with seven sublaminates of four plies using continuum shell elements (SC8R) (more details in the Abaqus Analysis User's Manual). The interlayer damage (delamination) was simulated in the present model with four layers of cohesive elements (COH3D8) of zero thickness using shared nodes method using Quads criterion for damage initiation and Benzeggagh-Kenane criterion ($\alpha = 1.6$) for damage propagation. The intralayer damage (matrix cracking and fiber failure) was modelled using Abaqus built-in Hashin damage model for damage initiation and linear energy law for damage propagation.

In addition, higher mesh density has been performed in an area close to the impact point because the existence of small cohesive elements size lead otherwise in convergence problems. Finally, the same softened penalty algorithm mentioned above for the specimens (pressure-overclosure) was applied in order to define the contact force diagram.

5.2 Experimental Test

Low velocity impact test was conducted in a laminated composite plate using an INSTRON Dynatup 9250 HV drop tower while the mass of the impactor was 16.7 kg using a hemispherical impactor of radius 8 mm. During the experiment the values of contact force, impactor deflection and impact energy as a function of time were defined. In addition, a fully

Table 3 Material properties

Ply mechanical properties Hexply IM7/8552

Density	$1590 \cdot 10^{-9} \text{ kg/mm}^3$
Ply thickness	0.125 mm
Elastic properties	$E_{11} = 155 \text{ GPa}$, $E_{22} = 8.4 \text{ GPa}$, $G_{12} = 3.2 \text{ GPa}$, $\nu_{12} = 0.3$
Ply strength properties	$X_T = 2200 \text{ MPa}$, $X_c = 1100 \text{ MPa}$, $Y_T = 25 \text{ MPa}$, $Y_c = 140 \text{ MPa}$, $S_L = 76 \text{ MPa}$, $S_T = 56 \text{ MPa}$

constrained boundary condition in the middle of all edges of the plate with a width of 30 mm (Fig. 2) was applied during impact.

The plate was tested with energy of 20 J which means that impactor velocity was 1.537 m/s.

6 Laminated Composite Stiffened Panel

6.1 Numerical Impact Modeling

An aerospace laminated composite stiffened panel [31] is depicted in Fig. 3 with skin thickness of 2 mm which is stiffened with omega stringers with 1.5 mm thickness and also contains three metallic frames made of aluminum with 3 mm thickness. The panel was manufactured with plies of UD composite material type IM7–8552 (by Hexcel). The skin laminate is $[45^\circ/90^\circ/-45^\circ/0^\circ/45^\circ/90^\circ/-45^\circ/0^\circ]_S$ and that of the stringers is $[45^\circ/-45^\circ/0^\circ_2/90^\circ/0^\circ]_s$.

In order to analyze a low velocity impact event on the laminated composite stiffened panel presented above, a model was created in Abaqus/CAE and analyzed using ABQUS/Explicit. The skin was modelled by the use of four sublaminates of continuum shell elements (SC8R) with four nodes and reduced integration while stringers with only one sublaminate. The same

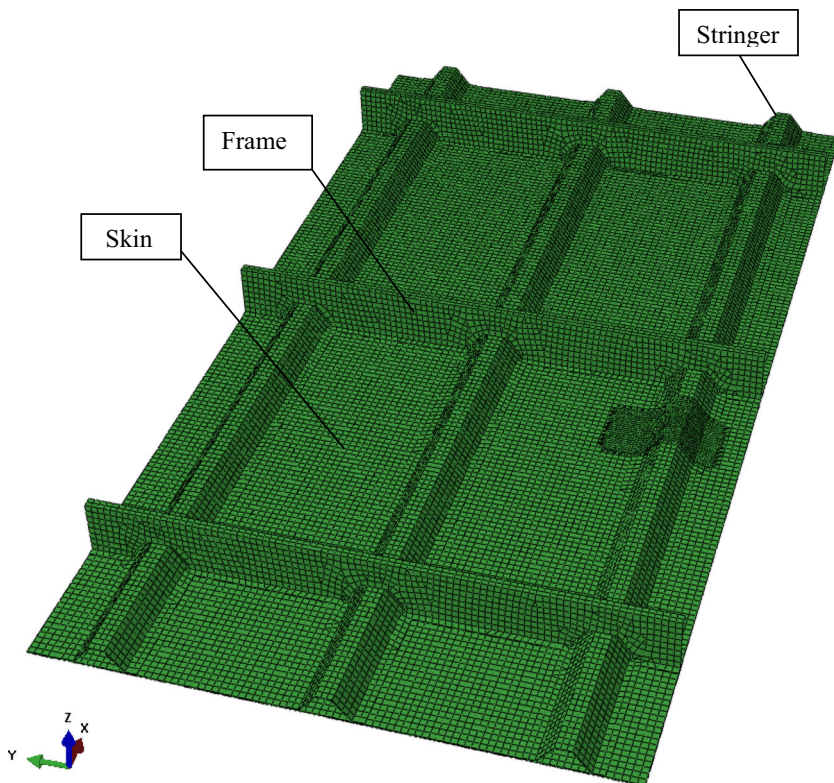


Fig. 3 Finite Element model of composite stiffened panel

criteria with composite plate for both interlayer and intralaminar damage initiation and propagation were considered in the present model. In addition two layers of cohesive elements (COH3D8) of zero thickness using shared nodes method were induced. Moreover, higher mesh density has been created in an area close to the impact point because the existence of small cohesive elements size leads in convergence problems during simulation and a finer mesh is mandatory.

General contact with hard contact law was used between the surfaces of the impactor and the first composite layer.

6.2 Experimental Test

A low velocity impact test was performed at the area of skin - stringer with the use of an INSTRON Dynatup 9250 HV drop tower, with impactor velocity $V_0 = 2.51$ m/s and mass of 16.7 kg. As a result, a BVID (Barely Visible Impact Damage) site was created at the specified location using a hemispherical impactor with a diameter of 16 mm (Fig. 4). Fully constrained boundary conditions at the large sides of the panel were used during the impact event.

7 Results and Discussion

7.1 Laminated Composite Specimens

Firstly, it is important to evaluate the behavior of specimens and understand the influence of all affecting parameter checking if delamination is created under impact loading. As a result impactor force and displacement of specimens in undamaged state have been calculated using

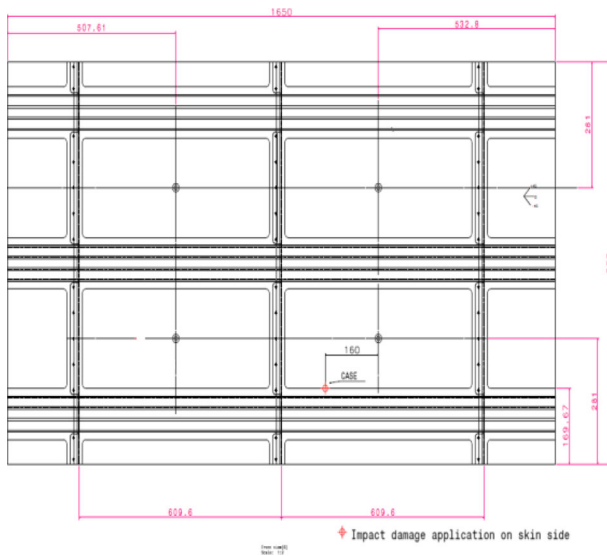


Fig. 4 Low velocity impact location for laminated composite stiffened panel

approaches of simplified analytical models with the help of MATLAB software (Fig. 5a and b).

From the force figures above the resulting maximum value for each impact energy is greater than 8.34 kN which is the damage critical value for the creation of a delamination according to Eq. (8) with $n_d = 1$. As a result, the existence of delamination is obvious for all impactor velocities because maximum load for all cases are higher than the interlaminar damage limit value.

Furthermore, for each case a comparison between numerical simulation and published experimental test results has been executed for both impact force and energy absorbed versus time. According to Soutis et al. [6] the kinetic energy of the impactor is transferred to the specimen during contact. An amount of this energy is absorbed from the composite as elastic deformation, while a larger part is dissipated due to intralaminar and interlaminar damage and friction between the contact bodies and among the plies of the layup. This energy transfer finishes when the value of the impactor velocity becomes zero and the impactor rebounds as a result of the flow of absorbed elastic energy from the specimen back to it. In conclusion, the absorbed energy by the specimen becomes a constant value due to damage and friction.

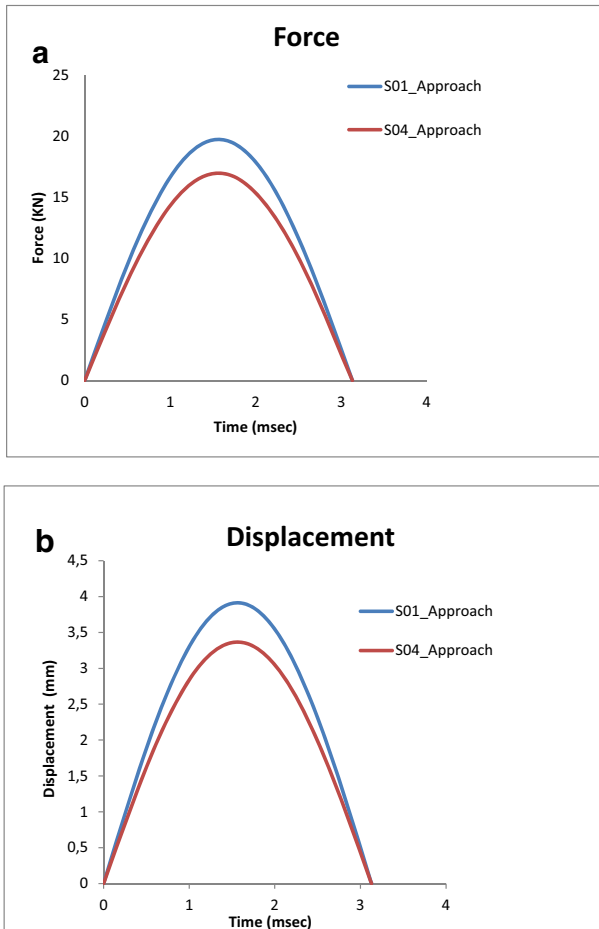


Fig. 5 Results of approaches for impact behavior

Firstly, the case of highest impactor velocity (Fig. 6) has been modelled using the following element types and damage models:

1. Continuum shell elements (SC8R) with induced cohesive elements for modelling both intralaminar (Hashin model for damage initiation and linear damage evolution) and interlaminar (Abaqus cohesive elements) damage.
2. Only continuum shell elements (SC8R) for intralaminar damage (Hashin model for damage initiation and linear damage evolution).
3. Conventional shell elements (S4R) simulating only intralaminar damage (Hashin model for damage initiation and linear damage evolution).
4. Solid elements (C8D8R) with VUMAT user subroutine modelling only intralaminar damage (Hashin model for fiber damage and Puck model for matrix damage).

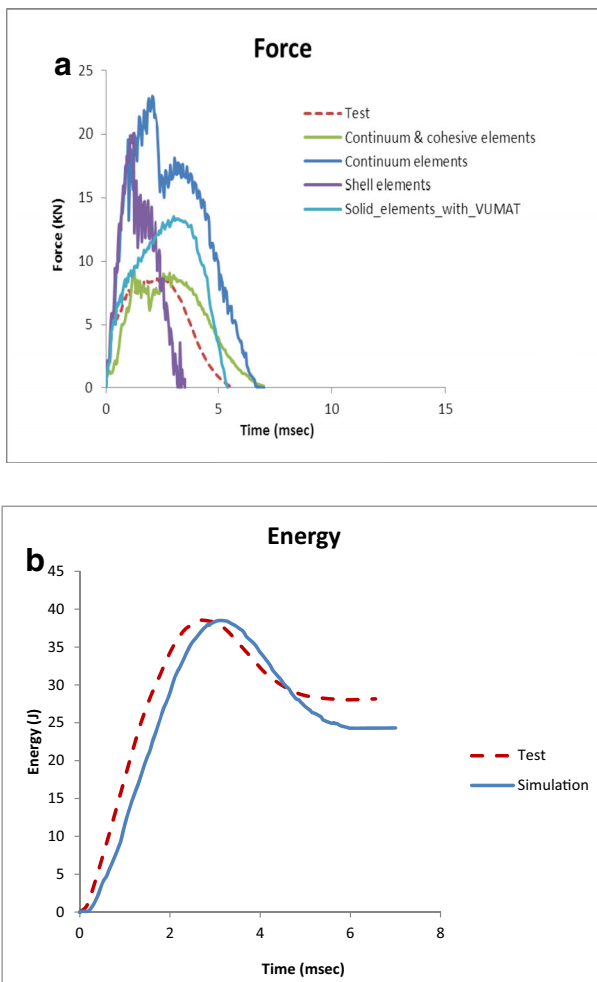


Fig. 6 **a** Force – time results for S01 specimen – Comparison of different methods of simulation **b** Energy – time results for S01 specimen (continuum & cohesive elements)

The comparison of all these different methods for the first case led to the conclusion that impact force for all the above methodologies, except for the first one, was overestimated probably due to increased transverse stiffness (conventional shell and solid elements). Only continuum shell elements with induced cohesive elements results are very close to experimental tests for both force and energy absorbed versus time. This result can be firstly explained due to the fact that delamination damage needs to be modelled as it is appeared between the plies of different orientation which has also been verified with the use of previously referred simplified analytical method and testing. In addition, continuum shell elements have better behavior and give more accurate response than conventional shells when impact is examined because they take into account contact of both sides and thickness difference. Finally, continuum shell elements capture more accurately the through-thickness response for composite laminate structures in comparison with solid elements.

Moreover, the conclusion of better results of continuum shell elements with induced cohesive elements was checked for the second case. Figure 7 confirms that this

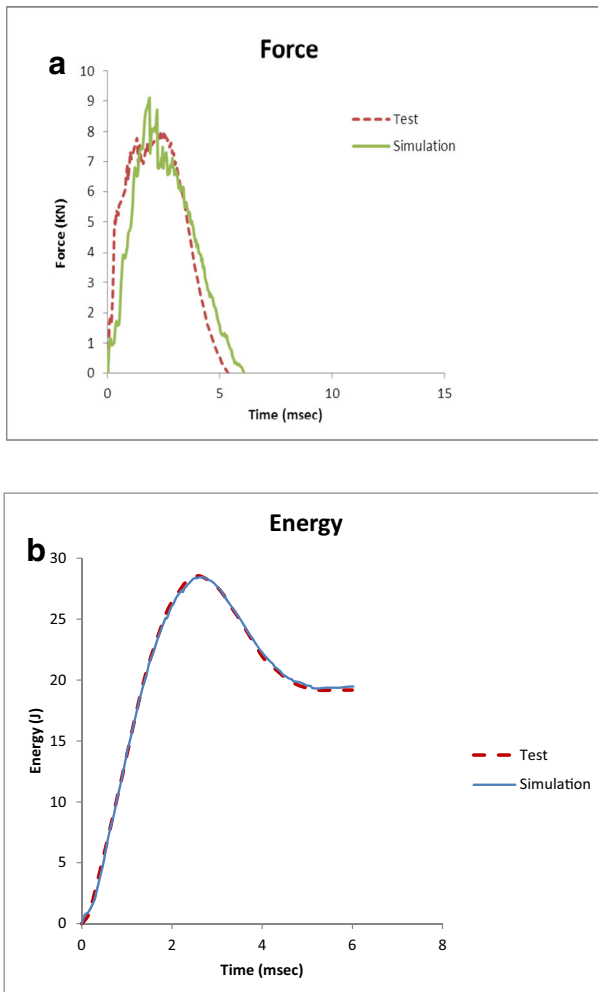


Fig. 7 **a** Force – time results for S04 specimen **b** Energy – time results for S04 specimen

methodology is more accurate as it is compared with experimental results of different impact velocity value.

7.2 Laminated Composite Plate

The case of low velocity impact of laminated composite plate (Fig. 8a) showed that simulation results are very close to performed experimental test. A force versus time graph confirms the accuracy of simulation results with the use of continuum shell elements with induced cohesive elements. Prediction of impactor force and total contact duration was enough accurate which means that there was a good estimation of the plate and contact stiffness.

In addition, the simulation results for matrix damage (Fig. 9a) and delamination between the sub-laminates (Fig. 9b) are very close to the experimental damage extension (Fig. 10) for the case of composite plate.

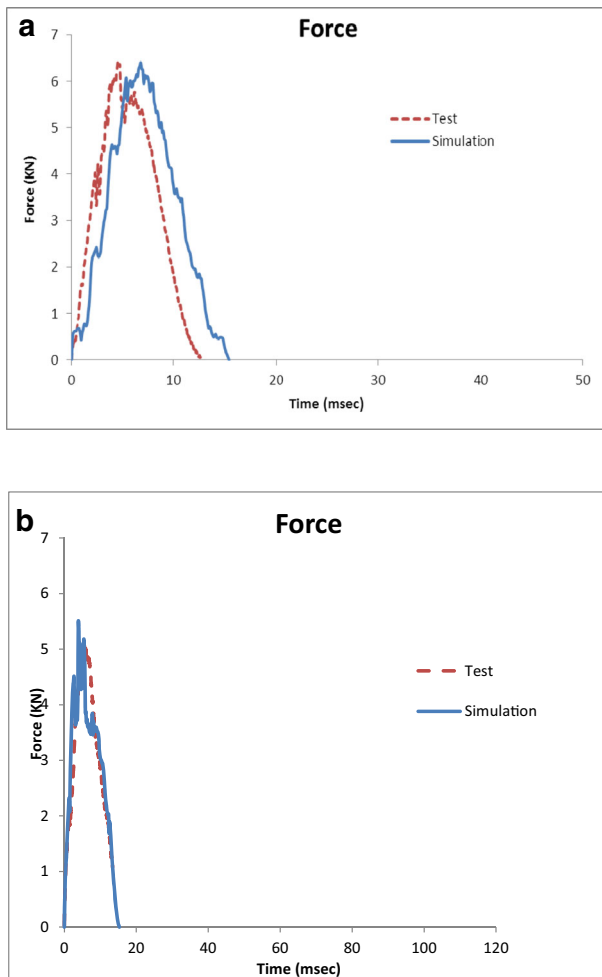


Fig. 8 **a** Force – time results of composite plate ($V_0 = 1.537$ m/s) **b** Force – time results of composite stiffened panel ($V_0 = 2.51$ m/s)

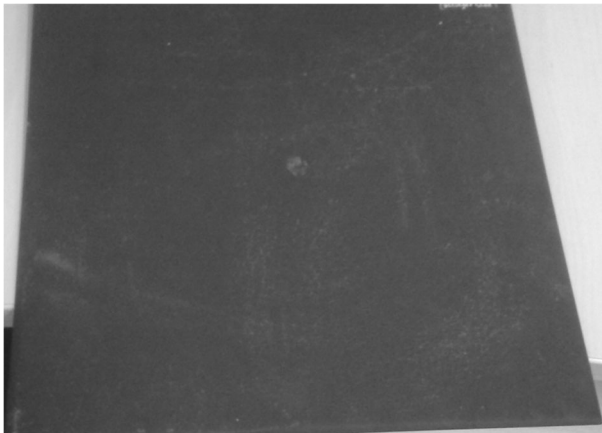


Fig. 10 Damage of composite plate due to low velocity impact (testing)

8 Conclusion

The aim of the presented paper is to study low velocity impact according to building block approach on laminated composite specimens, a plate and an aerospace stiffened panel. In order to make it feasible, a validation of experimental data with simplified models for quick estimation and numerical results has been executed. These numerical methodologies include simulation with conventional shell elements, continuum shell

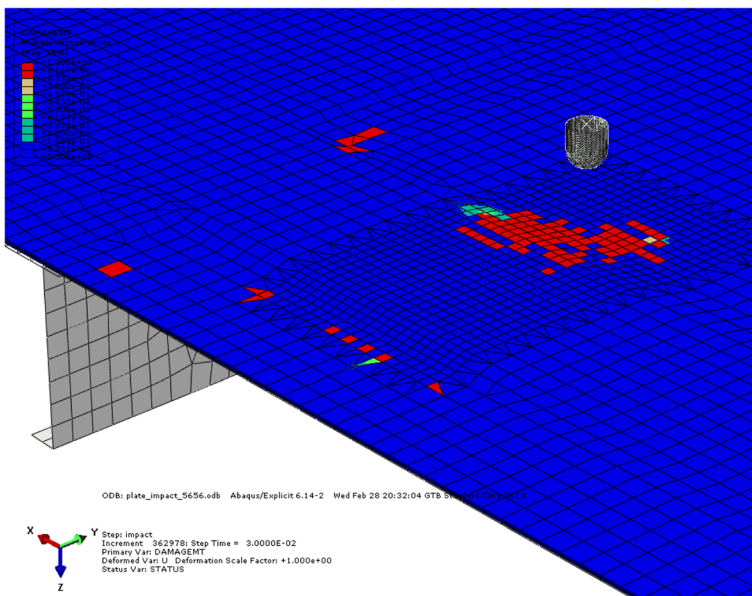
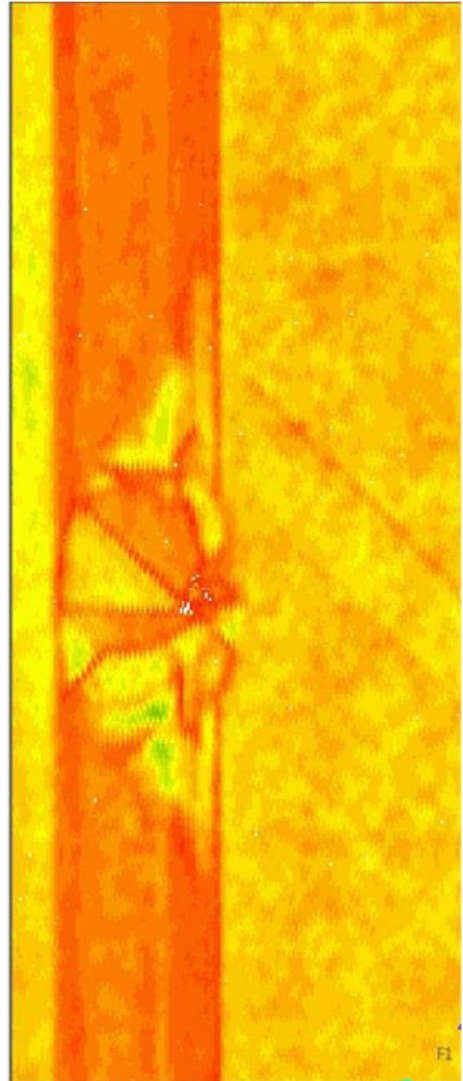


Fig. 11 Matrix damage in tension – aerospace composite stiffened panel (skin – stringer area)

Fig. 12 C-scan (skin – stringer area)



elements with and without the existence of cohesive elements for delamination, solid elements with the use of a user subroutine. The comparison of the impact force and the absorbed energy versus time for all mentioned simulation techniques showed that continuum shell elements with induced cohesive elements for delamination modelling give the most accurate simulation results. Finally, the analysis for the mode and magnitude of damage in the simulation activities of composite plate and aerospace composite stiffened panel enforce the conclusion of accurate results using continuum shell elements and cohesive elements for interlaminar damage.

Compliance with Ethical Standards

Conflict of Interest Non declared.

References

1. Bikakis, G.S.E.: Simulation of the dynamic response of GLARE plates subjected to low velocity impact using a linearized spring-mass model. *Aerosp. Sci. Technol.* **64**, 24–30 (2017)
2. Tsamasphyros, G.J., Bikakis, G.S.: Analytical modeling to predict the low velocity impact response of circular GLARE fiber–metal laminates. *Aerosp. Sci. Technol.* **29**(1), 28–36 (2013)
3. Giannopoulos, I.K., Theotokoglou, E.E., Zhang, X.: Impact damage and CAI strength of a woven CFRP material with fire retardant properties. *Compos. Part B.* **91**(April), 8–17 (2016)
4. Olsson, R.: Impact response of composite laminates – a guide to closed form solutions. FFA-TN 1992–33. The Aeronautical Research Institute of Sweden, Bromma (1993)
5. Abrate, S.: Modeling of impacts on composite structures. *Compos. Struct.* **51**(2), 129–138 (2001)
6. Shi, Y., Soutis, C.: A finite element analysis of impact damage in composite laminates. *Aeronaut. J.* **116**(1186), 1331–1347 (2012)
7. Shi, Y., Pinna, C., Soutis, C.: Modelling impact damage in composite laminates: a simulation of intra- and inter-laminar cracking. *Compos. Struct.* **114**, 10–19 (2014)
8. Shi, Y., Soutis, C.: Modelling low velocity impact induced damage in composite laminates. *Mech. Adv. Mater. Mod. Process.* **3**, 14 (2017)
9. Olsson, R.: Closed form prediction of peak load and delamination onset under small mass impact. *Compos. Struct.* **59**(3), 341–349 (2003)
10. Christoforou, A.P.: Impact dynamics and damage in composite structures. *Compos. Struct.* **52**(2), 181–188 (2001)
11. Abrate, S.: Impact on composite structures. Cambridge University Press, Cambridge (1998)
12. Davies, G.A.O., Zhang, X., Zhou, G., Watson, S.: Numerical modelling of impact damage. *Composites.* **25**(5), 342–350 (1994)
13. Elder, D.J., Thomson, R.S., Nguyen, M.Q., Scott, M.L.: Review of delamination predictive methods for low speed impact of composite laminates. *Compos. Struct.* **66**(1–4), 677–683 (2004)
14. Olsson, R.: Mass criterion for wave controlled impact response of composite plates. *Compos. A: Appl. Sci. Manuf.* **31**(8), 879–887 (2000)
15. Gonzalez, E.V., Maimi, P., Camanho, P.P., Lopes, C.S., Blanco, N.: Effects of ply clustering in laminated composite plates under low-velocity impact loading. *Compos. Sci. Technol.* **71**, 805–817 (2011)
16. Olsson, R.: Analytical prediction of large mass impact damage in composite laminates. *Compos. A: Appl. Sci. Manuf.* **32**(9), 1207–1215 (2001)
17. Shivakumar, K.N., Elber, W., Illg, W.: Prediction of impact force and duration due to low velocity impact on circular composite laminates. *J. Appl. Mech.* **52**(3), 674–680 (1985)
18. Yigit, A.S., Christoforou, A.P.: Limits of asymptotic solutions in low-velocity impact of composite plates. *Compos. Struct.* **81**(4), 568–574 (2007)
19. Olsson, R., Donadon, M.V., Falzon, B.G.: Delamination threshold load for dynamic impact on plates. *Int. J. Solids Struct.* **43**(10), 3124–3141 (2006)
20. Reddy, J.N.: Theory and Analysis of Elastic Plates and Shells. Taylor and Francis, Philadelphia (2007)
21. Christoforou, A.P., Yigit, A.S.: Effect of flexibility on low velocity impact response. *J. Sound Vib.* **217**(3), 563–578 (1998)
22. Hashin, Z.: Failure criteria for unidirectional fiber composites. *J. Appl. Mech.* **47**, 329–334 (1980)
23. Abaqus v6.14 analysis user's guide. Dassault Systèmes Simulia Corp., Providence (2014)
24. ABAQUS/Explicit VUMAT for the simulation of damage and failure in unidirectional fiber composite materials, ABAQUS Answer 3123, Simulia (2011)
25. Puck, A., Schürmann, H.: Failure analysis of FRP laminates by means of physically based phenomenological models. *Compos. Sci. Technol.* **58**(7), 1045–1067 (1998)
26. Puck, A., Schürmann, H.: Failure analysis of FRP laminates by means of physically based phenomenological models. *Compos. Sci. Technol.* **62**(12–13), 1633–1662 (2001)

27. Perillo, G., Vedvik, N.P., Echtermeyer, A.T.: Numerical analysis of low velocity impacts on composite. Advanced modelling techniques. Proc. Simulia. Conf. (2012)
28. Sharif-Khodaei, Z., Ghajari, M., Aliabadi, M.: Determination of impact location on composite stiffened panels. *Smart Mater. Struct.* **21**(10): 105026 (2012)
29. ASTM D7136/D7136M-05: Standard test method for measuring the damage resistance of a fiber-reinforced polymer matrix composite to a drop-weight impact event. ASTM International, West Conshohocken, PA, USA (2005)
30. Tsampas Spyridon, Analysis of compression failure in multidirectional laminates, Phd Thesis, Imperial College (2013)
31. Tserpes, K.I., Karachalios, V., Giannopoulos, I., Prentzias, V., Ruzek, R.: Strain and damage monitoring in CFRP fuselage panels using fiber Bragg grating sensors. Part I: design, manufacturing and impact testing. *Compos. Struct.* **107**: 726–736 (2014)